

Calculation of the photoabsorption coefficient in a hot and dense aluminum plasma

David Salzmänn*

Soreq Nuclear Research Center, Yavne, Israel

Göran Wendin

Institute of Theoretical Physics, Fack, S-40220 Göteborg 5, Sweden

(Received 20 March 1978)

The photoabsorption coefficient of high-temperature (10^2 – 10^5 eV) and high-density (10^{20} – 10^{22} cm $^{-3}$) aluminum plasma in the range of $h\nu = 10^2$ – 10^5 eV is calculated. The calculation uses detailed configuration accounting. The photoabsorption mechanisms included are the photoelectric effect, inverse bremsstrahlung, Compton effect, and bound-bound photoexcitation. The Stark broadening of the sharp-line and the absorption-edge structure is properly taken into account and its influence versus ion density is shown. The sensitivity of the results to changes in the various parameters is discussed.

I. INTRODUCTION

The effort concentrated in recent years on the research into hot and dense plasmas, particularly laser-produced plasmas, have stimulated the theoretical and experimental investigation of x-ray production and reabsorption in these plasmas. The estimates of the conversion rate of the incoming laser energy into x-ray energy ranges from a few percent¹ to 40%–50%,^{2,3} depending on the atomic number of the target, laser pulse shape, and energy. This means that x-ray production is not a subsidiary effect but one of the major factors in the energy balance in the plasma.

X-rays also have special importance as a major diagnostic tool of the plasma. X-ray emission is a primary process occurring during both the evolution and expansion phases of the plasma. In fact, it is the main detectable process carrying information on the plasma during the stage of plasma production and heating. From the emerging x-ray spectrum information about the electron temperature, ion density, and ionization state distribution can be unfolded. However, since the x-ray spectrum undergoes reabsorption inside the plasma, a good calculation of the absorption coefficient is required for plasma simulations in order to obtain a unique interpretation of the experimental results. In the present report we describe a calculation of the absorption coefficient of hot and dense aluminum plasma for x-ray energies from 10^2 to 10^5 eV.

In spite of its importance only a few works were published on the subject of x-ray absorption coefficients in hot dense plasmas. Calculations for dense Be and Ge plasmas⁴ as well as Al plasma⁵ were published by Rozsnyai. The main differences between his calculation⁵ and the present work can be summarized as follows. (a) The calculations of Rozsnyai use the "average atom" (AA) approxi-

mation,⁴ whereas in the present work a "detailed configuration accounting" (DCA) is applied. In DCA the exact atomic parameters of the levels are used for the calculations⁶ of the cross sections as well as the equation of state of the plasma. (b) In the AA approximation a Boltzmann-type population distribution in the excited levels is assumed. This is true only at high-density LTE plasmas. At lower densities, when the plasma still obeys a quasi-steady state,⁷ the ground state is overpopulated, altering the total absorption cross sections accordingly.

In these respects DCA is preferable over the AA approximation. The limitations of DCA are the following: (i) for the use of DCA a complete set of atomic data for the constituents of the plasma is required and these are available only for a limited number of atoms.⁶ For the others, these data sets must be computed separately if DCA is used in the calculations; (ii) the atomic data sets used in the DCA method were calculated for isolated atoms and ions only. The effect of the plasma microfields on these atomic parameters is negligible only at low-density plasmas where these fields cannot alter significantly the bound electron wave functions. At high densities the alteration of the atomic parameters (levels' energies, cross sections, and rate coefficients) must be incorporated properly, thereby complicating the DCA method. Since the AA approximation treats the bound and free electrons together in the frame of a self-consistent-field calculation it is applicable also in the high-electron-density regime where the DCA method is not practical anymore.

Experimentally it was found that the x-ray spectrum radiated by intermediate- Z laser produced plasmas in the practically achievable temperature and density region is concentrated around 1 keV,² a region in which the photoelectric effect dominates the absorbing processes. Photoelectric ab-

sorption is certainly the most important absorptive process in aluminum plasmas for temperatures and densities in the range of interest of the present work. Nevertheless, to obtain the total absorption coefficient three other processes must be incorporated into the calculation. These are inverse bremsstrahlung which affects mainly the low-energy portion of the spectrum, the Compton effect which is significant only close to the 100-keV limit, and line absorption which is effective mainly below the absorption edges.

II. PHOTOELECTRIC EFFECT

The photoelectric effect is the major absorptive process in the keV domain, and it is very sensitive to the partial densities of the various ionization states. The total photoelectric absorption coefficient μ_{ph} is composed of the partial absorption cross sections of the various ionization states. These may be either in their ground states or in one of their excited states.

$$\mu_{ph} = \sum_{k=0}^Z (n_{k,g} \sigma_{k,g} + n_{k,e} \sigma_{k,e}). \quad (1)$$

$n_{k,g}$ and $n_{k,e}$ are the partial densities of the k th ion in the ground and excited states, respectively $\sigma_{k,g}$ and $\sigma_{k,e}$ are the corresponding cross sections. For the calculation of the cross sections only the K and L electrons were taken into account. For these cross sections, averages were taken over the initial states and summed over all allowed final states. Neglecting the contribution of M and higher-shell electrons is justified by the relatively low cross section of these electrons in the range of interest of the present work and by the relatively low partial density of these electrons in the plasma. M electrons may have some effect at the very-low-energy part of the spectrum, but as in this domain other absorptive processes dominate (mainly inverse bremsstrahlung), their influence on the total absorption coefficient is probably negligible.

The partial densities were taken from a previous work,⁷ where these densities were calculated by assuming a quasi steady state in the plasma. The processes which account for the equilibrium in the plasma are electron impact ionization, radiative, dielectronic, and three-body recombinations. The calculation includes also the effect of ionization potential reduction and a proper population-distribution function of the excited states. However, the calculation disregards the possibility of electron degeneracy thereby restricting the range of validity of the results to not too high electron densities, i.e., $n_e \leq 5.3 \times 10^{21} T_e^{3/2}$ (n_e in cm^{-3} , T_e in eV).

The photoelectric cross sections were calculated

using the Hartree-Fock (HF) method. The ground and bound excited states of the aluminum ions were calculated in the average-of-configuration HF approximation. At low electron densities (much below solid-state densities) the free-electron contribution to the ionic potential can be neglected and the ions can be treated as free. The continuum wave functions were calculated in the average-of-configuration HF potential of the frozen ionic core with the ionized orbital removed.⁸ This approach can be expected to give a good description of the gross features of the total cross section. For the inner shells, the nuclear potential dominates the behavior and many electron corrections should be very small, except perhaps near the ionization thresholds.

The corresponding cross sections are published for neutral aluminum in Ref. 9. Our results for the low-ionization states were compared to the results in this reference. The comparison showed agreement to within 5% for the energy range included in our study.

An illustrative example of the calculated absorption coefficients is shown in Fig. 1. The graphs exhibit the features expected on intuitive grounds for the photoelectric cross section. First, the shell structure of the absorption coefficient is clearly shown. Second, as the temperature increases, the L electrons are first stripped off the ions with a corresponding decrease of the absorption coefficient in the low-energy portion of the spectrum. The stripping of K electrons starts at about $T_e = 300$ eV above which there is a decrease of μ_{ph} for photon energies above the K edge as well.

III. INVERSE BREMSSTRAHLUNG, COMPTON EFFECT, AND LINE ABSORPTION

The absorption by inverse bremsstrahlung is important only for low-energy photons. In fact, the absorption coefficient for this absorption process decreases proportionally¹⁰ to $(h\nu)^{-3}$,

$$\mu_{ib} = 2.44 \times 10^{-37} Z^2 n_T n_e [1/T_e^{1/2} (h\nu)^3] \text{ cm}^{-1}. \quad (2)$$

Here T_e is the electron temperature in eV, n_T and n_e are the total ion and electron densities, respectively.

The Compton absorption by free electrons affects only the high-energy portion of the absorption coefficient. It was calculated by means of the well-known Klein-Nishina formula.¹¹

The discrete photoexcitation absorption coefficient was calculated by¹²

$$\mu_1 = (1/8\pi)(g_n/g_m)\lambda^2 n_{j_m} h A_{j, nm} P(E). \quad (3)$$

Here g_n and g_m are the statistical weights of the up-

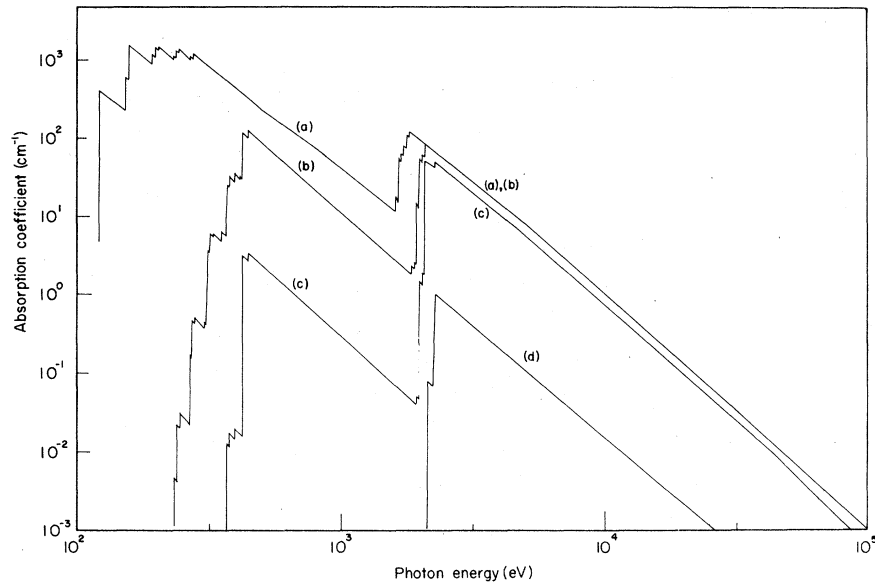


FIG. 1. Photoelectric absorption coefficient of aluminum plasma with ion density of 10^{21} cm^{-3} and electron temperatures of (a) 32 eV, (b) 100 eV, (c) 320 eV, and (d) 1000 eV.

per and lower states, respectively, λ is the wavelength of the transition (in cm), n_{jm} is the density of the lower state, $A_{j,nm}$ is the Einstein coefficient of the transition, and $P(E)$ is the line-profile function.

Figure 2 shows the relative effect of the four absorption processes for an aluminum plasma with $T_e = 300 \text{ eV}$ and $n_T = 10^{21} \text{ cm}^{-3}$, where for the sake of illustration we have suppressed the broadening of the absorption lines. It can be seen from Fig. 2, that the photoelectric effect is the major absorptive process above the L -absorption edge, i.e., above 200–400 eV, the exact limit depends on the ionization states that are present in the plasma. Below the L edges inverse bremsstrahlung absorption dominates. The inclusion of line

broadening alters this conclusion as the absorption by line wings, not too far from the lines' centers may be much higher than inverse bremsstrahlung absorption. The Compton effect is negligible almost everywhere, except perhaps in the high-energy limit of the graph where its value is about 8% of the total absorption coefficient.

IV. LINE BROADENING

The line-broadening mechanism considered in this work is the dipole Stark broadening as this was found to be the principal line-broadening process in aluminum plasmas,⁵ in the temperature, and in density domains of this work. In fact, at $T_e = 300 \text{ eV}$, $n_T = 10^{21} \text{ cm}^{-3}$ the dipole Stark broaden-

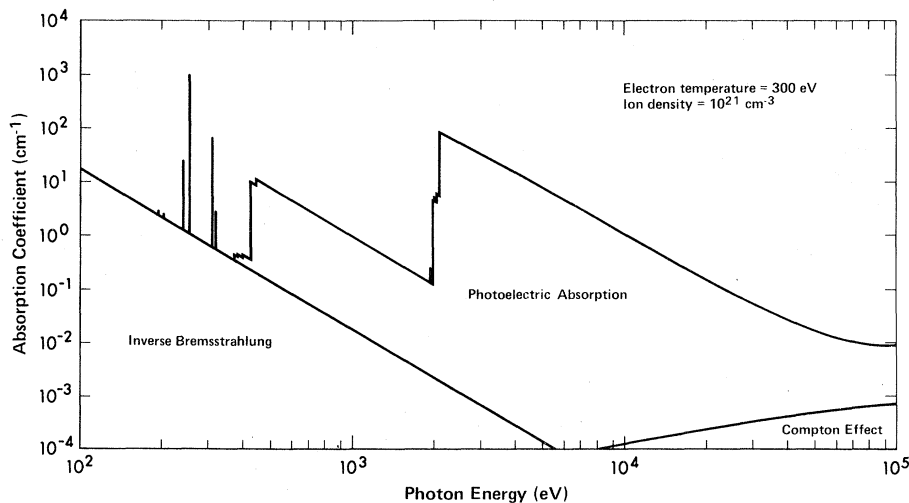


FIG. 2. Total absorption coefficient at $T_e = 300 \text{ eV}$ and $n_T = 10^{21} \text{ cm}^{-3}$. The relative contribution of the various absorption mechanisms is exhibited.

ing of the Lyman- α transition in H-like ions, is about⁵ 0.68 eV, compared to 0.017 eV for electron-impact broadening and 0.22 eV for the Doppler linewidth. Similar relations hold for other absorption lines. The exact line profile is a convolution of a Gaussian-type profile, whose width is the Doppler linewidth, with a Lorentzian profile (impact broadening) and the correct Stark-profile functions. However, the last two profiles can be convolved to a good approximation into a Lorentzian profile having the Stark broadening as the characteristic width.⁴ This last one is then convolved with the Doppler line shape to produce a Voigt profile. The main property of the Voigt line shape is that close to the line center, the profile has approximately a Gaussian shape, whereas far from the center, the absorption follows approximately a Lorentzian function. The Gaussian portions of the lines are below the energy resolution of our calculations, as well as the corresponding line shifts, so only the Lorentzian line wings, with the Stark width were incorporated in our calculations. High-resolution absorption-line profile scans and line shifts require separate calculations. For the Stark width an approximate formula by Griem¹³ was used. Comparison to more refined calculations⁵ proved that this formula predicted reasonably accurate linewidths. It must also be noted that the photoelectric absorption spectrum should be "broadened" as the absorbing electron is initially in a Stark-broadened level. This broadening mechanism smooths out the sharp absorption edges. We found this effect to be important and interesting enough to be included in the calculations.

V. DISCUSSION

Figures 3, 4, and 5 show the absorption coefficients (in cm^{-1}) versus photon energy (in eV) for electron temperatures of 100, 300, and 1000 eV, and ion densities of 10^{20} , 10^{21} , and 10^{22} atoms per cm^3 . The most striking feature of the absorption coefficient is its great sensitivity to all these parameters.

The sensitivity versus photon energy is moderate between the highest L edge (of AlXI) at about 600 eV up to about 1200 eV, and again above the highest K edge at about 2300 eV. In these regions the absorption coefficients vary proportionally to $(h\nu)^{-\alpha}$ with $\alpha \cong 3.0$ in the lower and $\alpha \cong 2.8$ in the upper region. However, immediately below the edges (about 200–600 eV and 1200–2000 eV) where photoexcitation is the principal absorption mechanism, the absorption coefficient is a sharply fluctuating function of the photon energy, in some cases with order of magnitude variations per eV energy interval. Very careful calculations are necessary in these regions to get reliable results.

Temperature variations affect the absorption coefficient through changing the ionization-distribution of the plasma,⁷ therefore its effect is maximum near the photoexcitation and absorption-edge regions. In these regions the absorption coefficient is a very sensitive function of the temperature. For example, for a 10^{20}-cm^{-3} aluminum plasma around $h\nu = 257$ eV, where the $2s^2S-3p^2P$ transition of AlXI has a large cross section, the total absorption coefficient varies from 84.3 cm^{-1} at $T = 30$ eV to 371 cm^{-1} at $T = 100$ eV, down to 0.422 cm^{-1} at $T = 300$ eV and 0.0121 cm^{-1} at $T = 1000$ eV, reflecting the variation in the relative

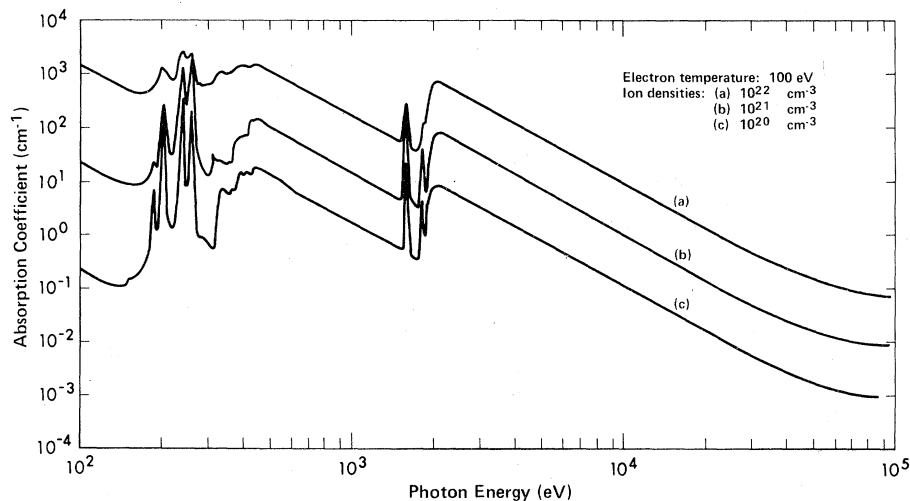


FIG. 3. Total absorption coefficient at $T_e = 100$ eV and ion densities of (a) 10^{22} cm^{-3} , (b) 10^{21} cm^{-3} , (c) 10^{20} cm^{-3} . The photoexcitation cross-sections are broadened by the dipole Stark effect.

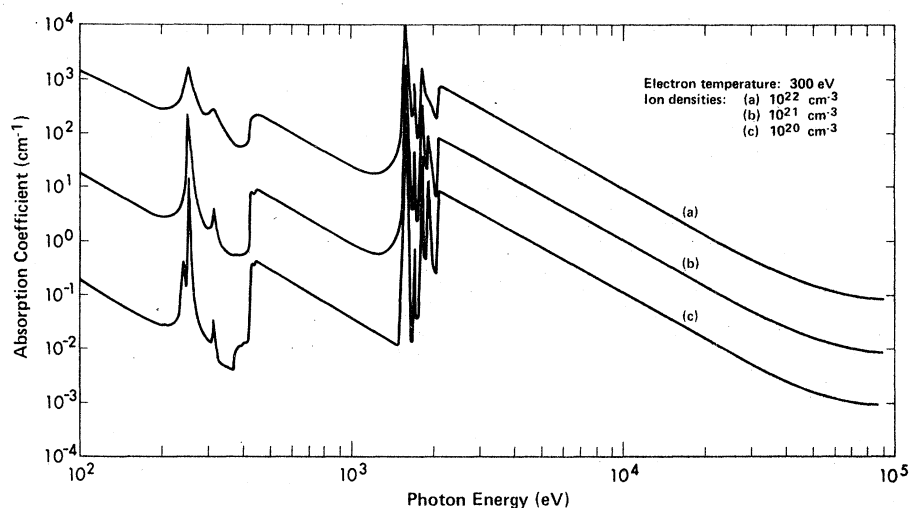


FIG. 4. Same as Fig. 3 at $T_e = 300$ eV.

density of Al XI in the plasma. Similarly, at the same density, around $h\nu = 1598$ eV, i.e., near the maximum for the $1s^2-1s2p$ photoexcitation in He-like aluminum, the absorption coefficient varies as follows: 1.05 cm^{-1} at $T = 30$ eV, 22.4 cm^{-1} at $T = 100$ eV, 220 cm^{-1} at $T = 300$ eV, and 35.5 cm^{-1} at $T = 1000$ eV.

Ion-density variations affect the absorption coefficient in three ways: (a) increasing the ion density increases the absorption coefficient proportionately, Eq. (1); (b) the ionization-state densities are determined by the total ion density. The average degree of ionization decreases with increasing density,⁷ and (c) the Stark broadening of the lines is determined mainly by the total ion density in the plasma varying approximately as¹³ $n_I^{2/3}$. The effect of line broadening at high densities is clearly shown in Figs. 3–5. At high ion densities the ab-

sorption coefficient is smoothed out due to this effect, particularly the fluctuating portions below the edges. Therefore, the variations versus photon energy at high densities are much smaller than in lower densities. In principle, at high enough densities all the line structure will disappear resulting in a smooth, slowly varying absorption function. However, for aluminum, this occurs only at impractically high densities.

In this work the photoabsorption coefficient of high-temperature and high-density aluminum plasma in the range of 10^2 – 10^5 eV was calculated using detailed configuration accounting (DCA). Special attention was given to get reasonably accurate and reliable results. Particularly, the photoelectric effect, which is the dominant absorption mechanism in the range considered in this work, was calculated to high precision. The absorption

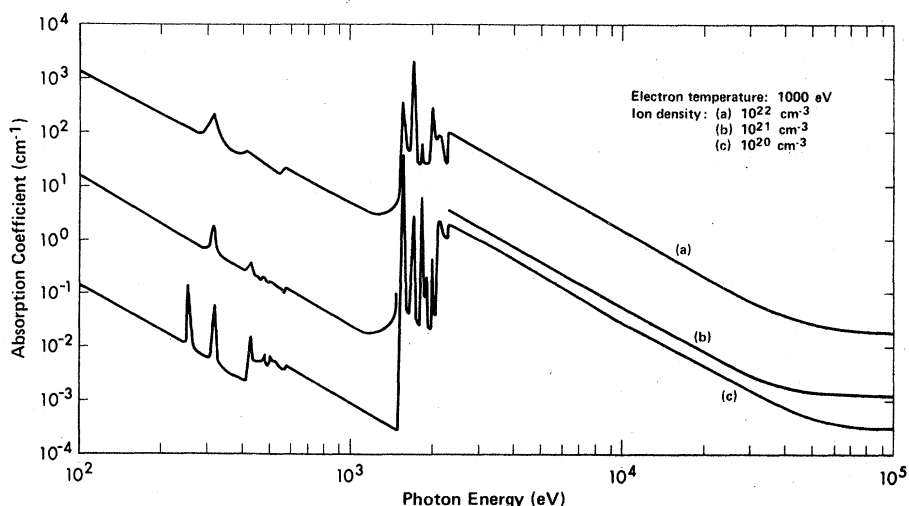


FIG. 5. Same as Fig. 3 at $T_e = 1000$ eV. For clarity, the highly fluctuating portion of curve (b) between 1500 and 2300 eV is omitted.

coefficient is dependent on several factors, a few of which were calculated to a few percent precision (cross sections of the photoelectric effect, Compton effect, and integrated line absorption cross section). Some others were calculated with less accuracy (10%–25%). These are the ionization state distribution⁷ and the linewidths.^{4,13} As the main influence of these two parameters is highest near and below the absorption edges, we expect moderate inaccuracies in our results in these regions. Improvement of the results in these regions requires separate research. In the regions where the absorption coefficient varies slowly, we believe that our results are accurate to a few percent.

ACKNOWLEDGMENTS

This work was initiated when the authors took part in a CECAM workshop in Orsay, France. The authors would like to thank Dr. Carl Moser, director of CECAM, for providing a stimulating scientific environment which was the starting point to this and other works. The final calculations were completed in the University of Alberta, where one of us (D.S.) is on a sabbatical leave. He would like to thank Professor A.A. Offenberger and the Department of Electrical Engineering of the University for their generous hospitality and for helping to finish this work.

*On sabbatical leave at the University of Alberta, Edmonton, Alberta, Canada.

¹M. J. Bernstein and G. G. Comisar, *J. Appl. Phys.* **41**, 729 (1970).

²P. J. Mallozzi *et al.*, *J. Appl. Phys.* **45**, 1891 (1974).

³K. G. Whitney, and J. Davis, *Appl. Phys. Lett.* **24**, 509 (1974).

⁴B. F. Rozsnyai, *J. Quant. Spectrosc. Radiat. Transfer* **17**, 77 (1977).

⁵B. F. Rozsnyai, "Temperature and Density Effects on Spectral Lines in Hot Dense Plasma," UCRL-78909 (1977).

⁶W. L. Wiese, M. W. Smith, and B. M. Miles, "Atomic Transition Probabilities," *Natl. Stand. Ref. Data Ser.*, *Natl. Bur. Stand.* **22** (1969).

⁷D. Salzmänn and A. D. Krumbein, *J. Appl. Phys.*

49, 3229 (1978).

⁸G. Wendin, *J. Phys. B* **4**, 1080 (1971); *Vacuum Ultraviolet Radiation Physics*, edited by E. E. Koch, R. Haensel, and C. Kunz (Pergamon Vieweg, New York, 1974) p. 225.

⁹R. H. Pratt, A. Ron, and H. K. Tseng, *Rev. Mod. Phys.* **45**, 273 (1973).

¹⁰Ya. B. Zeldovich and Yu. P. Raiser, *Elements of Gas-dynamics and the Classical Theory of Shock Waves* (Academic, New York, 1968), Vol. I.

¹¹K. Siegbahn, *Alpha-, Beta-, and Gamma-ray Spectroscopy* (North-Holland, Amsterdam, 1965).

¹²J. Richter, in *Plasma Diagnostics*, edited by Lochte-Holtgreven (North-Holland, Amsterdam, 1968).

¹³H. R. Griem, *Spectral Line Broadening by Plasmas* (Academic, New York, 1974).